

Fermi National Accelerator Laboratory

FERMILAB-Conf-98/190-E

CDF

D0

The Dijet Differential Cross Section, M_{jj} and α_s

F.S. Chlebana

For the CDF and D0 Collaborations

*Fermi National Accelerator Laboratory
P.O. Box 500, Batavia, Illinois 60510*

June 1998

Published Proceedings of the *33rd Rencontres de Moriond: QCD and High Energy Hadronic Interactions*,

Les Arcs, France, March 21-28, 1998

Disclaimer

This report was prepared as an account of work sponsored by an agency of the United States Government. Neither the United States Government nor any agency thereof, nor any of their employees, makes any warranty, expressed or implied, or assumes any legal liability or responsibility for the accuracy, completeness, or usefulness of any information, apparatus, product, or process disclosed, or represents that its use would not infringe privately owned rights. Reference herein to any specific commercial product, process, or service by trade name, trademark, manufacturer, or otherwise, does not necessarily constitute or imply its endorsement, recommendation, or favoring by the United States Government or any agency thereof. The views and opinions of authors expressed herein do not necessarily state or reflect those of the United States Government or any agency thereof.

Distribution

Approved for public release; further dissemination unlimited.

Copyright Notification

This manuscript has been authored by Universities Research Association, Inc. under contract No. DE-AC02-76CHO3000 with the U.S. Department of Energy. The United States Government and the publisher, by accepting the article for publication, acknowledges that the United States Government retains a nonexclusive, paid-up, irrevocable, worldwide license to publish or reproduce the published form of this manuscript, or allow others to do so, for United States Government Purposes.

The Dijet Differential Cross section, M_{jj} and α_s

F.S. Chlebana

*Fermi National Accelerator Laboratory, MS 318, P.O. Box 500,
Batavia, IL, 60510*

A preliminary measurement of the inclusive dijet differential cross section obtained from $p\bar{p}$ collisions at $\sqrt{s} = 1.8$ TeV by the CDF collaboration is presented. Results are presented from CDF and DØ for the the dijet mass distribution and compared to QCD calculations. The effect of changing the renormalization scale and the choice of the parton density functions on the predicted cross section is shown. An estimate of α_s is obtained from the inclusive jet data.

1 Introduction

The production of collimated hadronic jets at high energy colliding-beam facilities has proven to be a rich source of tests for QCD, the fundamental theory of the strong interactions. Theoretical developments in both perturbative Next-to-Leading Order (NLO) and shower Monte Carlo calculations now permit rapid calculation of many QCD jet processes with theoretical uncertainties small enough to allow detailed comparison with measured spectra¹. There are now available numerous parton distribution functions (PDF's) which utilize large ensembles of experimental data from deep inelastic scattering and direct photon production to provide unbiased estimates of the gluon and quark distributions of the nucleon. These PDFs form an essential component of jet production calculations.

Recent measurements of the inclusive jet differential cross section from CDF have indicated an excess of events at high E_T when compared to the QCD predictions with standard parton distributions. This excess has generated a great deal of theoretical interest. Quark substructure would lead to deviations from QCD at high E_T . A measurement of dijet angular distributions tests the properties of parton-parton scattering without a strong dependence on the choice of the PDF. Such measurements have been used to set limits on quark compositeness². Another possible explanation for the excess is the gluon distribution being larger than expected at high x .

1.1 The Inclusive Dijet Differential Cross Section

Preliminary results for the triple differential jet cross section, $d\sigma/(dE_T d\eta_1 d\eta_2)$ are presented by the CDF collaboration. Jets are identified by a cone algorithm with cone radius \mathcal{R} defined as $\mathcal{R} = \sqrt{(\Delta\phi)^2 + (\Delta\eta)^2} = 0.7$. The transverse energy is calculated from $E_T = E \sin\theta$, where the energy E is the scalar sum of energy in the calorimeter towers within the cone, and θ is the angle formed by the event vertex, the beam direction and the cone center. Events are collected by on-line identification of at least one jet with transverse energy above thresholds of 20, 50, 70, and 100 GeV. The 20, 50, and 70 GeV samples were prescaled by factors of 1000, 40, and 8

respectively. No prescale was applied to the 100 GeV trigger sample. The data sample presented here correspond to an integrated luminosity of 86 pb^{-1} from $\sqrt{s} = 1.8 \text{ TeV}$ $p\bar{p}$ collisions taken during the 1994-1995 Fermilab Tevatron Collider run. The analysis includes events with at least two reconstructed jets. The *trigger* jet is required to satisfy $E_T > 40 \text{ GeV}$ and to be within the central pseudorapidity region, $0.1 < |\eta_1| < 0.7$. The *probe* jet is required to satisfy $E_T > 10 \text{ GeV}$ and to sit in one of four pseudorapidity bins, $0.1 < |\eta_2| < 0.7$, $0.7 < |\eta_2| < 1.4$, $1.4 < |\eta_2| < 2.1$ or $2.1 < |\eta_2| < 3.0$.

The well-understood response properties of the CDF central calorimeter are utilized to measure the E_T of the *trigger* jet. The measured energies are corrected for detector resolution and smearing using the same procedure used in the measurement of the inclusive jet cross section³. The cross section is measured as a function of the trigger jet's E_T . Four separate distributions are determined corresponding to the four bins of η_2 . The preliminary results are presented in Figure 1 and compared to the calculated cross section determined using JETRAD⁴ with several different PDFs. The data are in good quantitative agreement with the QCD predictions except at high E_T . The error bars represent the statistical errors. The systematic errors are currently being finalized.

In order to emphasize the high E_T region the cross sections have been scaled by E_T^n using a different exponent for each of the η_2 bins. The results are shown in Figure 2. Preliminary results from run Ia are also included and are seen to be in good agreement with the run Ib results. The data tend to be higher than that expected from existing PDFs at high E_T . The CTEQ4HJ⁶ PDF results in a better agreement with the data at high E_T .

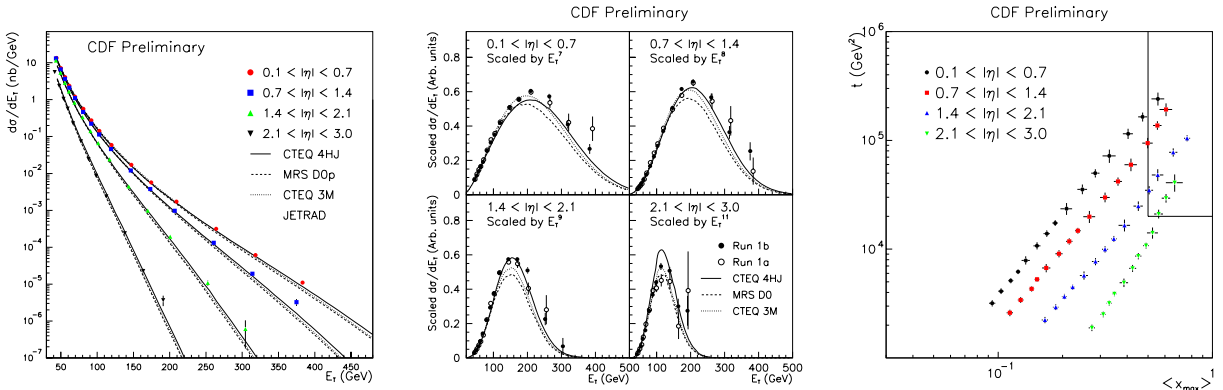


Figure 1: The preliminary measurement of the dijet triple differential cross section. The results are compared to the predictions of JETRAD using different PDFs.

Figure 2: The differential dijet cross section for the four η bins scaled by E_T^n where n is specified on the plots.

Figure 3: The x_{\max} and \hat{t} region probed by the dijet triple differential cross section measurements. The upper right corner shows the high x and high Q^2 region.

The E_T and pseudorapidities of the leading jets are related to the momentum fraction, x , of the partons involved in the interaction. In leading order the relation is

$$x_1 = \frac{E_T}{\sqrt{s}}(e^{\eta_1} + e^{\eta_2}); \quad x_2 = \frac{E_T}{\sqrt{s}}(e^{-\eta_1} + e^{-\eta_2}). \quad (1)$$

For fixed E_T and η_1 , different momentum fractions can be selected by requiring that the *probe* jet lie in different η intervals. We define x_{\max} as the maximum of x_1 and x_2 . For a two body process one intuitive choice for the QCD scale of the interaction is

$$Q^2 \sim -\hat{t} = 2E_T^2 \cosh^2 \eta^* (1 - \tanh \eta^*) \quad (2)$$

The data have been converted from (E_T, η_2) bins to (x_{\max}, \hat{t}) bins and shown in Figure 3. The high E_T region of the inclusive jet cross section distribution corresponds to high x . We also see

that the events occur at high Q^2 . In contrast to the inclusive jet data which yield information along a line in the $x - Q^2$ plane the dijet data provide information over a region of the $x - Q^2$ plane. The dijet data will prove useful as input in NLO QCD fits to determine new sets of PDFs.

1.2 The Dijet Invariant Mass Distribution

Both CDF and DØ have measured the differential dijet mass cross section, $\Delta d\sigma^2/\Delta M_{jj}d\eta_1d\eta_2$ as a function of the dijet mass. The preliminary CDF measurement is based on 87 pb^{-1} . A cone algorithm with a fixed cone size of $\mathcal{R} = 0.7$, is used to reconstruct jets. The two leading jets are required to be within the central region and satisfy $|\eta| < 2$. In order to ensure a high trigger efficiency over the entire dijet mass range both jets are required to satisfy $|\cos\theta^*| < 2/3$ where $\cos\theta^* = \tanh\eta^*$ with $\eta^* = (\eta_1 - \eta_2)/2$. Additional cuts were applied to reduce background. The measured jet energies are corrected for detector and smearing effects. The dijet mass is determined from the 4-vector definition

$$M_{jj} = \sqrt{(E_1 + E_2)^2 - (\vec{p}_1 + \vec{p}_2)^2}, \quad (3)$$

where E is the jet energy and \vec{p} is the jet 3-momentum.

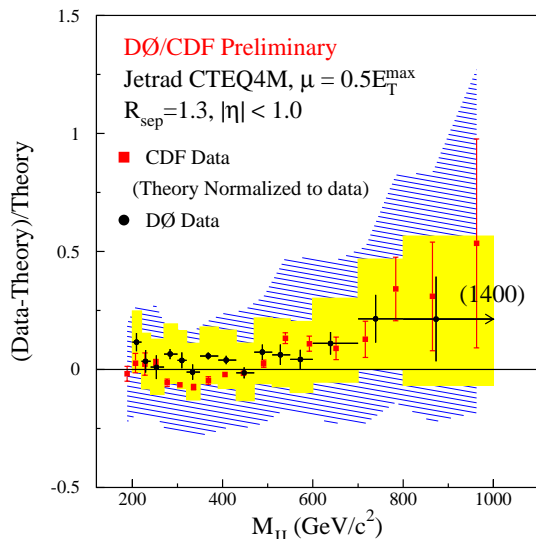


Figure 4: Comparison of the preliminary dijet mass distributions from CDF and DØ compared with theory predictions using JETRAD with the CTEQ4M PDF.

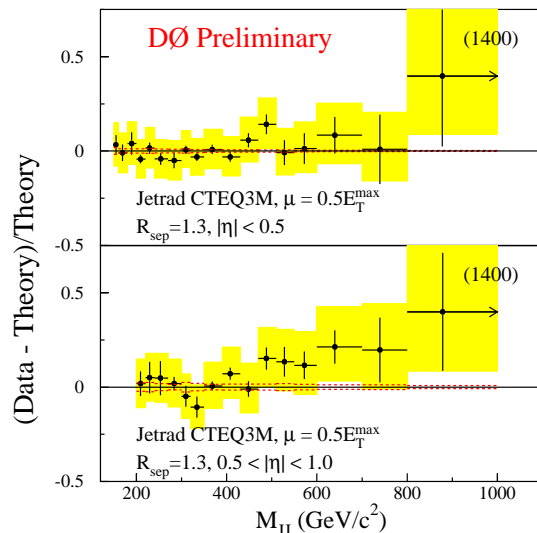


Figure 5: The preliminary DØ dijet mass distributions for central ($|\eta| < 0.5$) and forward ($0.5 < |\eta| < 1.0$) jets compared with the QCD calculation.

The DØ measurement requires that both jets satisfy $|\eta| < 1$. The dijet mass is calculated assuming massless jets from

$$M_{jj}^2 = 2E_T^{(1)} E_T^{(2)} (\cosh(\Delta\eta) - \cos(\Delta\phi)). \quad (4)$$

The difference in the calculated mass using the different mass definitions is a few percent. Preliminary results from both experiments are compared to the QCD prediction determined using JETRAD with $\mu = 0.5E_T^{max}$, $R_{sep} = 1.3$ and the CTEQ4M PDF in Figure 4. The CDF data are shown as squares and has been normalized to the theory prediction in the first six bins. The inner shaded band shows the systematic error on the DØ measurement while the outer band represents the error on the CDF measurement. The shape of the distributions measured by the two collaborations are in excellent agreement.

DØ has split the sample into two η regions. The top plot of Figure 5 compares the measured cross section as a function of M_{jj} for $|\eta| < 0.5$ to the theory expectation while the bottom plot shows the results for $0.5 < |\eta| < 1.0$. The data are consistent with the theory predictions however the data tend to be somewhat higher than the expectation at high E_T for the case of more forward jets.

The effect of changing the renormalization scale is shown in Figure 6. The DØ data are used in the ratio (Data-Theory)/Theory where the theory calculation was performed using JETRAD with CTEQ3M⁸ and $\mu = 0.5E_T^{max}$. The renormalization scale has been varied from $0.25E_T^{max}$ to $2E_T^{max}$ and compared to the nominal case with $\mu = 0.5E_T^{max}$. The effect of changing the renormalization scale shows up as a shift in the cross section with a slight M_{jj} dependence. The result of changing the PDF is shown in Figure 7. The ratio of (Data-Theory)/Theory is plotted using the DØ data compared to the calculation of JETRAD with CTEQ3M. The difference in the cross section obtained using the MRSA'⁷, CTEQ4HJ and CTEQ4M PDF is shown. The choice of the PDF can result in significant change in the shape.

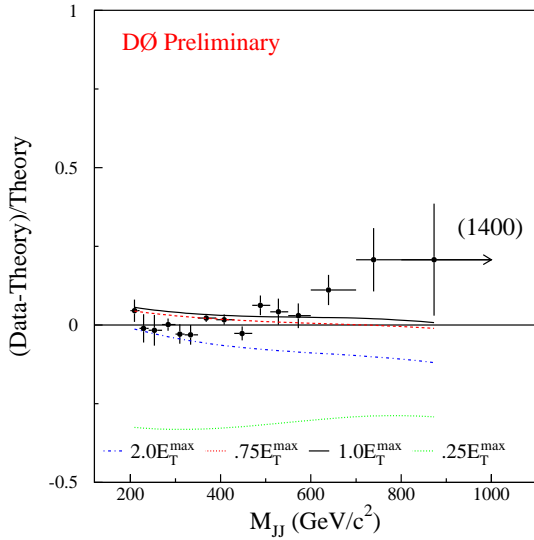


Figure 6: The DØ data are compared to the QCD predictions of JETRAD with $\mu = 0.5E_T^{max}$. The curves show the effect of changing the renormalization scale from $0.25E_T^{max}$ to $2E_T^{max}$. The jets are required to satisfy $|\eta| < 1$.

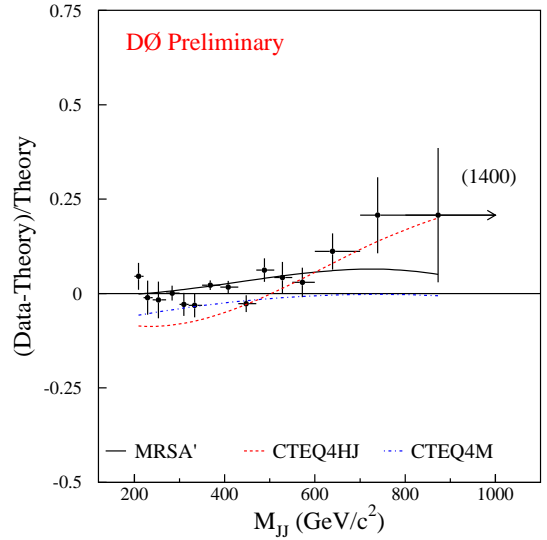


Figure 7: The DØ data are compared to the QCD predictions of JETRAD using the CTEQ3M PDF. The curves show the change in the cross section obtained using different PDFs. The jets are required to satisfy $|\eta| < 1$.

1.3 An Estimate of α_s

The CDF collaboration has used the method described by Giele *et al.*⁵ to determine α_s from the inclusive jet data. The NLO QCD inclusive cross section can be expressed as

$$\frac{d\sigma(E_T)}{dE_T} = \alpha_s^2(\mu_R)A(E_T) + \alpha_s^3(\mu_R)B(E_T). \quad (5)$$

The constants A and B can be calculated from QCD and assuming a particular PDF set and value of $\alpha_s \equiv \alpha_s(M_Z)$. The program JETRAD was used to determine the coefficients. For each bin in E_T $\alpha_s(E_T)$ is determined and translated to α_s using

$$\alpha_s(M_Z) = \frac{\alpha_s(\mu_R)}{1 - \alpha_s(\mu_R)L(\lambda)} \quad (6)$$

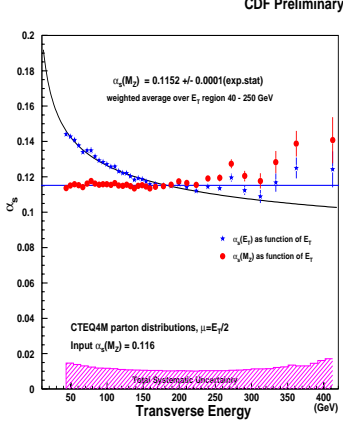


Figure 8: The α_s as determined from the CDF inclusive jet data using the CTEQ4M PDF.

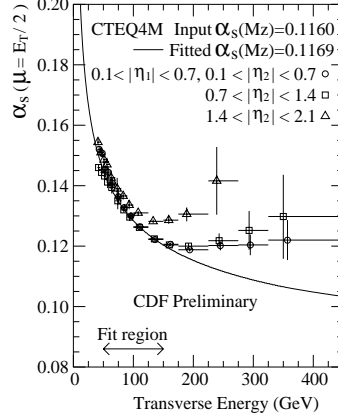


Figure 9: The α_s determined from the CDF dijet data using the CTEQ4M PDF.

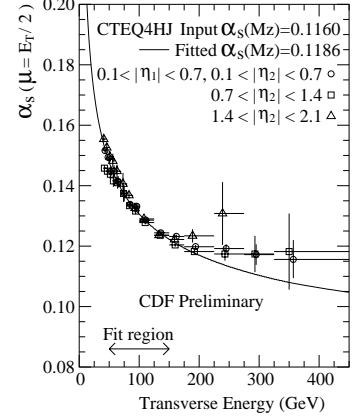


Figure 10: The α_s determined from the CDF dijet data using the CTEQ4HJ PDF.

with

$$L(\lambda) = (b_0 + b_1 \alpha_s) \log(\lambda), \quad (7)$$

where b_0 and b_1 are known.

The coupling constant was determined from the measurement of the inclusive jet cross section over the E_T range of 40 to 250 GeV. The results are shown in Figure 8. The stars show the value of $\alpha_s(E_T)$ and demonstrate the running of α_s . The circles represent the value of α_s translated to M_Z using Equation 6. The error bars represent the statistical errors and the systematic error is shown as the hatched band at the bottom of the plot. The results obtained are dependent on the PDF used to calculate the constants and the value of α_s used in the calculation. When using CTEQ4M with $\alpha_s(M_Z) = 0.116$ the value of $\alpha_s = 0.1152 \pm 0.0001$ is determined.

The same method was used with the dijet data. The result for CTEQ4M is shown in Figure 9 and the CTEQ4HJ result is shown in Figure 10. The error bars represent only the statistical errors. The region over which the data are fit to get extract α_s is shown in the plots. The CTEQ4HJ PDF results in a better agreement with the data at high E_T . The correlation between α_s and the gluon distribution makes an independent determination of α_s difficult.

2 Conclusions

The differential dijet cross section can be used as an input to global QCD fits. Unlike the inclusive jet cross section which provides information along a line in the $x - Q^2$ plane the dijet differential cross section provides information over a region in the $x - Q^2$ plane. The extended $x - Q^2$ coverage allows the possibility to better determine the shape of the PDFs from global QCD fits. The region of most interest is the high E_T region or equivalently high x and high Q^2 . We have seen that a modified PDF can account for some of the excess of events observed at high E_T .

The dijet mass spectrum is seen to be in agreement with QCD predictions. The shape of the data from CDF and $D\bar{O}$ are consistent. We have seen that changing the input parameters to the theory calculation can result in a significant change in the expected cross section.

An estimate of α_s using the inclusive jet data has been presented. The method is dependent on the choice of the PDF and starting value of α_s used to determine the constants in Equation 5.

Acknowledgments

We thank the staffs at Fermilab and the collaborating institutions for their contributions to this work, and acknowledge support from the Department of Energy and the National Science Foundation (U.S.A.), Commissariat à L'Energie Atomique (France), State Committee for Science and Technology and Ministry for Atomic Energy (Russia), CNPq (Brazil), Departments of Atomic Energy and Science and Education (India), Colciencias (Columbia), CONACyT (Mexico), Ministry of Education and KOSEF (Korea), and CONICET and UBACyT (Argentina).

References

1. Ellis S. et al., *Phys. Rev. Lett.* **64**, 2121 (1990); Giele W.T. et al., *Nucl. Phys. B* **403**, 633 (1993).
2. F. Abe et al., CDF Collab., *Phys. Rev. Lett.* **77**, 5336 (1996).
3. F. Abe et al., CDF Collab., *Phys. Rev. Lett.* **77**, 438 (1996).
4. Giele W.T., Glover E.W.N. and Kosower D.A. *Phys. Rev. Lett.* **73**, 2019 (1994).
5. Giele W.T. et al., *Phys. Rev. D* **53**, 120 (1996).
6. H.L. Lai et al., CTEQ Collab., *Phys. Rev. D* **55**, 1280 (1997).
7. A.D. Martin et al., *Phys. Rev. D* **51**, 4756 (1995).
8. H.L. Lai et al., CTEQ Collab., *Phys. Rev. D* **51**, 4763 (1995).